

## A NOTE ON TRAVELLING WAVES IN COMPETITIVE REACTION SYSTEMS

LAWRENCE K. FORBES<sup>1</sup>

(Received 5 March, 2013; revised 26 August, 2013; first published online 26 November, 2013)

### Abstract

This note considers an established reaction–diffusion model for a combustion system, in which there are competing endothermic and exothermic reaction pathways. A combustion front is assumed to move at constant speed through the medium. An asymptotic theory is presented for solid fuels in which material diffusion is ignored, and it allows a simple and complete analysis of the approximate system in the phase plane. Both the adiabatic and nonadiabatic cases are discussed.

2010 *Mathematics subject classification*: 80A30.

*Keywords and phrases*: combustion model, competing reactions, travelling wave, asymptotic analysis, phase plane.

### 1. Introduction

Travelling waves are now a well-established phenomenon in reaction–diffusion systems, in a variety of applications. Mathematically they are interesting because they predict the wave behaviour typical of hyperbolic partial differential equations, but in systems that are parabolic. The famous Fisher wave is an example of such behaviour in a biological system, as discussed by Murray [9]. Travelling waves also occur in combustion systems, and have been the subject of intense interest. Gray and Scott [6] and Zel’dovich et al. [13] discuss further examples of these phenomena.

There has also been recent interest in chemical combustion systems in which both exothermic (heat-producing) and endothermic (heat-consuming) reactions occur simultaneously. In a model of bushfire spread, Forbes [3] appealed to such competitive mechanisms in an attempt to explain why it is that not every small heat input develops into a major conflagration. Ball et al. [1] undertook a comparative study of reactions with parallel and competing pathways. The idea of reactions in which endothermic and exothermic mechanisms are in competition has been developed more recently by

---

<sup>1</sup>School of Mathematics and Physics, University of Tasmania, Private Bag 37, Hobart, Tasmania 7001, Australia; e-mail: [Larry.Forbes@utas.edu.au](mailto:Larry.Forbes@utas.edu.au).

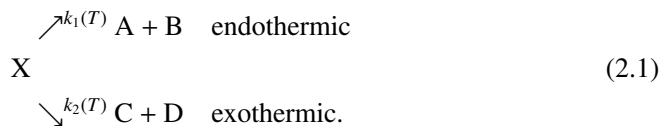
© Australian Mathematical Society 2013, Serial-fee code 1446-1811/2013 \$16.00

Hmaldi et al. [7] and analysed further by Sharples et al. [10], who included material diffusion.

In this note, the model of Hmaldi et al. [7] is simplified by means of an asymptotic approximation to the nonlinear temperature-dependent reaction rates. This permits the resulting system to be integrated once, with the result that the behaviour of the two possible steady states can be specified in advance, so as to guarantee conditions needed for a travelling combustion wave in the system. A reasonably straightforward phase-plane analysis then allows the complete determination of the travelling wave. That model is then extended to allow for nonadiabatic conditions in which cooling to ambient temperature is permitted, apparently for the first time, and a phase-plane approach is also shown to be possible in that situation.

## 2. Model and asymptotic analysis

Consider a system of two one-step chemical reactions, in which a single chemical species  $X$  decays either by an endothermic reaction to form products  $A$  and  $B$ , or else by an exothermic process to create species  $C$  and  $D$ . Schematically, this may be represented in the form



The “classical” combustion model consists only of the exothermic portion of this reaction, and has been studied by Weber et al. [11], and by Brindley et al. [2] for solid fuels of varying geometry. Ball et al. [1] refer to a scheme of the form (2.1) as a competitive reaction pathway, and the two reaction rates  $k_1(T)$  and  $k_2(T)$  are dependent on the reaction temperature  $T$ . From Hmaldi et al. [7] and Sharples et al. [10], the governing equations for the system are

$$\frac{\partial X}{\partial t} = D \frac{\partial^2 X}{\partial x^2} - Xk_1(T) - Xk_2(T), \quad (2.2)$$

$$\rho c_p \frac{\partial T}{\partial t} = K \frac{\partial^2 T}{\partial x^2} - \rho Q_1 Xk_1(T) + \rho Q_2 Xk_2(T). \quad (2.3)$$

Here  $X$  and  $T$  are the mass fraction and temperature, respectively, and  $\rho$  is the density of the material. The constant  $c_p$  is a heat capacity,  $D$  and  $K$  are mass and temperature diffusion coefficients, and  $Q_1$  and  $Q_2$  are enthalpies of reaction for the endothermic and exothermic reactions, respectively.

Nondimensional variables are introduced, and used henceforth. The reaction rates are assumed to obey Arrhenius kinetics

$$k_1(T) = Z_1 \exp\left(-\frac{E_1}{RT}\right), \quad k_2(T) = Z_2 \exp\left(-\frac{E_2}{RT}\right), \quad (2.4)$$

in which constants  $Z_1$  and  $Z_2$  are first-order rates with dimension 1/time, and  $E_1$  and  $E_2$  are activation energies for each reaction. The quantity  $E_2/R$  is then chosen as the scale for temperature, in which  $R$  is the universal gas constant. Lengths are scaled relative to the quantity  $\sqrt{(KE_2)/(\rho Q_2 Z_2 R)}$  and the unit of time is taken to be  $(c_p E_2)/(Q_2 Z_2 R)$ . The mass fraction  $X$  is dimensionless.

In these new variables, the mass and energy equations (2.2)–(2.3) take the form

$$\frac{\partial X}{\partial t} = \sigma \frac{\partial^2 X}{\partial x^2} - \alpha \mu X k_1(T) - \mu X k_2(T), \quad (2.5)$$

$$\frac{\partial T}{\partial t} = \frac{\partial^2 T}{\partial x^2} - \alpha \gamma X k_1(T) + X k_2(T), \quad (2.6)$$

in which the Arrhenius rate laws (2.4) reduce simply to  $k_1(T) = \exp(-\epsilon/T)$  and  $k_2(T) = \exp(-1/T)$ . The five dimensionless parameter groups appearing in (2.5)–(2.6) are

$$\alpha = \frac{Z_1}{Z_2}, \quad \gamma = \frac{Q_1}{Q_2}, \quad \epsilon = \frac{E_1}{E_2}, \quad \mu = \frac{c_p E_2}{Q_2 R}, \quad \sigma = \frac{\rho D}{K c_p}. \quad (2.7)$$

Following Hmadi et al. [7] and Sharples et al. [10], this note is concerned with travelling waves of constant dimensionless speed  $c$ , and, accordingly, the travelling-wave variable

$$\xi = x - ct \quad (2.8)$$

is introduced. To simplify matters, the coefficient  $\sigma$  of material diffusion in (2.5)–(2.7) is set to zero, as is appropriate for solid fuels [11].

The Arrhenius reaction rates (2.4) are somewhat unrealistic, in that they allow reaction to occur at any temperature above absolute zero; this is the famous “cold boundary difficulty”, and has been commented on by many authors, including Gray et al. [5] and Matkowsky and Sivashinsky [8]. Here, the approach of Forbes and Derrick [4] is adopted, and it is assumed that the reaction only occurs above some critical (“ignition”) temperature  $\theta_a$ , taken to be the same for both rates. A further discussion of this concept is given by Zel’dovich et al. [13]. As a result, the rates (2.4) are replaced with the dimensionless forms

$$k_1(T) = \begin{cases} 0 & T < \theta_a \\ 1 - e^{\epsilon(\theta_a - T)} & T > \theta_a, \end{cases} \quad k_2(T) = \begin{cases} 0 & T < \theta_a \\ 1 - e^{(\theta_a - T)} & T > \theta_a. \end{cases} \quad (2.9)$$

The asymptotic approximation now proceeds by simplifying the rates (2.9) using linearization, and assuming that the temperature always remains above the ignition value  $\theta_a$  (which consequently plays no further role in the problem). The rates are thus taken to be

$$k_1(T) \approx \epsilon T_1, \quad k_2(T) \approx T_1 \quad \text{where } T_1 = T - \theta_a, \quad (2.10)$$

for  $T$  moderately close to the ignition value  $\theta_a$ . The analysis to follow, then, may be regarded as a weakly nonlinear approximation. This is similar in some respects to the theory presented by Forbes and Derrick [4], which led to a classical “sech squared” soliton temperature profile in that application.

When the travelling-wave assumption (2.8) is combined with the asymptotic approximations (2.10), the partial differential equations (2.5)–(2.6) reduce to the simpler nonlinear third-order system of ordinary differential equations

$$-c \frac{dX}{d\xi} = -\lambda XT_1, \quad -c \frac{dT_1}{d\xi} = \frac{d^2T_1}{d\xi^2} + \delta XT_1, \quad (2.11)$$

in which it is convenient to define auxiliary constants

$$\lambda = \mu(\alpha\epsilon + 1), \quad \delta = 1 - \alpha\gamma\epsilon. \quad (2.12)$$

The two ordinary differential equations in the system (2.11) are combined in such a way as to eliminate the nonlinear product  $XT_1$ , and this leads at once to the equation

$$-c \frac{dT_1}{d\xi} = \frac{d^2T_1}{d\xi^2} + \frac{c\delta}{\lambda} \frac{dX}{d\xi}.$$

This can immediately be integrated, using the undisturbed boundary conditions  $X \rightarrow X_0$ ,  $T_1 \rightarrow 0$  as  $\xi \rightarrow \infty$  ahead of the propagating flame front. Here  $X_0$  denotes the original unburnt fuel concentration. As a result, an explicit relation is obtained for the mass fraction  $X$  in terms of perturbation temperature  $T_1$  in the form

$$X = X_0 - \frac{\lambda}{c\delta} \left[ cT_1 + \frac{dT_1}{d\xi} \right], \quad (2.13)$$

although the wave speed  $c$  is as yet undetermined. This relation (2.13) allows the mass fraction  $X$  to be eliminated from the second differential equation in the system (2.11), leading to the second-order differential equation

$$\frac{d^2T_1}{d\xi^2} = \left[ -c + \frac{\lambda}{c} T_1 \right] \frac{dT_1}{d\xi} - \delta X_0 T_1 + \lambda T_1^2 \quad (2.14)$$

for the perturbation temperature  $T_1(\xi)$ . Equation (2.14) thus represents a first integral of the original travelling-wave system (2.11).

### 3. Phase-plane analysis

The second-order equation (2.14) is easily seen to have two steady states, one at  $T_1 = 0$  and the other at  $T_1 = \delta X_0 / \lambda$ . For a travelling wave, it is required that  $T_1 = 0$  should correspond to the unburnt conditions ahead of the wave, as  $\xi \rightarrow \infty$ , so that the second steady state  $T_1 = \delta X_0 / \lambda$  must represent conditions far behind the wave, as  $\xi \rightarrow -\infty$ . For a wave travelling from left to right, there must be an elevated temperature behind the front, and as a result, it may be assumed that the auxiliary parameter  $\delta > 0$  in (2.12). Since  $T_1 > 0$ , this condition  $\delta > 0$  is thus a requirement for a travelling wave of this type. Finally, a genuine travelling wave requires this second steady state to be a saddle. The first steady state at  $T_1 = 0$  must be stable, and in fact must be chosen

to be a degenerate stable node; this is because the rate functions (2.9) are zero for  $T_1 < 0$ , and consequently the ignition value  $\theta_a$  is arbitrary. A similar choice was made by Weber et al. [11] for the corresponding point in their analysis.

The second-order equation (2.14) may now be analysed completely in the phase plane, by writing it in the equivalent form

$$\frac{dT_1}{d\xi} = F, \quad \frac{dF}{d\xi} = -\delta X_0 T_1 + \lambda T_1^2 + \left[-c + \frac{\lambda}{c} T_1\right] F. \quad (3.1)$$

It is now a routine matter to linearize about the two steady states for this system, to determine their nature.

For the steady state  $(T_1, F) = (0, 0)$  far ahead of the flame front, the eigenvalues are easily calculated to be

$$\frac{1}{2}[-c \pm \sqrt{c^2 - 4\delta X_0}].$$

As the ignition temperature  $\theta_a$  is arbitrary in this asymptotic approximation, this steady state must be a degenerate stable node, and this immediately leads to the formula

$$c = 2\sqrt{\delta X_0} \quad (3.2)$$

for the wave speed  $c$ . Consequently, the two steady states for the phase-plane system (3.1) have the following behaviour:

$$(T_1, F) = (0, 0), \quad \text{repeated eigenvalue } -c/2, \quad \text{eigenvector } \begin{bmatrix} 1 \\ -c/2 \end{bmatrix}, \quad (3.3)$$

and

$$(T_1, F) = \left(\frac{\delta X_0}{\lambda}, 0\right), \quad \text{eigenvalues } c/4, -c, \quad \text{eigenvectors } \begin{bmatrix} 1 \\ c/4 \end{bmatrix}, \begin{bmatrix} 1 \\ -c \end{bmatrix}, \quad (3.4)$$

in which the wave speed  $c$  is as given in equation (3.2).

Once the temperature  $T_1$  has been determined from the phase-plane system (3.1), the mass fraction  $X$  is then easily obtained from (2.13) in the form

$$X = X_0 - \frac{\lambda}{c\delta}[cT_1 + F]. \quad (3.5)$$

The differential equations (3.1) have been integrated in this note using the Runge–Kutta–Fehlberg package provided by Matlab, using the speed (3.2) and starting near the equilibrium point  $(T_1, F) = (\delta X_0/\lambda, 0)$ . It follows from equation (3.5) that, for the second steady state far behind the wave front, the mass fraction is  $X = 0$ , so that all the fuel is consumed by the flame.

Some sample results are presented here, for parameter values  $\alpha = 1/2$ ,  $\mu = 1$ ,  $\gamma = 1$ ,  $\epsilon = 3/2$  and unburnt mass fraction  $X_0 = 1$ . From equation (3.2), the resulting wave speed is thus  $c = 1$ . Figure 1(a) shows the temperature profile. As expected, there is a smooth wave front moving from left to right with speed  $c$ , such that the temperature

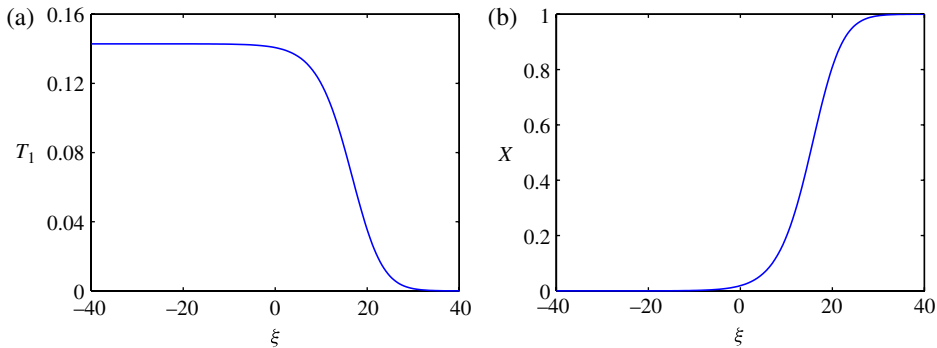


FIGURE 1. (a) Temperature profile and (b) mass fraction profile for a travelling wave, with parameters as given in the text.

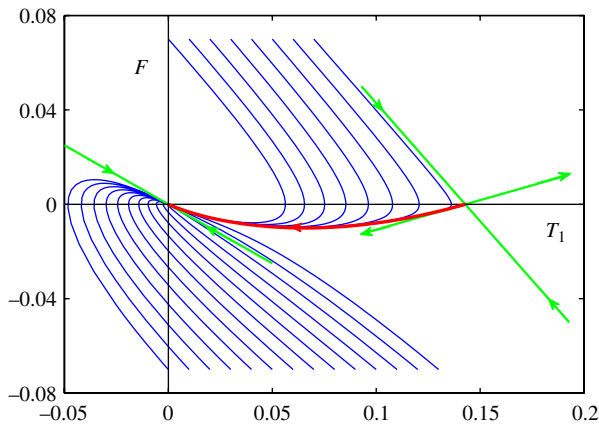


FIGURE 2. The phase plane showing the saddle at  $(\delta X_0/\lambda, 0)$  and the degenerate stable node at  $(0, 0)$ . The eigenvectors are shown with green arrows from the two points. The travelling wave is indicated with a red heavy solid line and other contours not associated with the travelling wave are added in blue. (Colour available online.)

profile decreases monotonically from the maximum value  $\delta X_0/\lambda$  behind the front to zero ahead of it. The mass fraction, computed from equation (3.5), is displayed in Figure 1(b). It increases monotonically from the burnt value zero behind the front to the unburnt value  $X_0 = 1$  ahead of it. These simple asymptotic results are in agreement with the profile shapes presented by Gray et al. [5] and Sharples et al. [10].

A complete view of the phase plane is shown in Figure 2 for this same case. These solution curves were obtained by numerical integration of the phase-plane system (3.1). A number of solution contours not associated with the travelling wave are sketched using thin solid lines, and these are all drawn into the degenerate stable node at  $(T_1, F) = (0, 0)$ , although the portions of these curves in the region  $T_1 < 0$  have no meaning, in view of the change of definition of the rates in (2.9). The special

contour, which starts at  $(T_1, F) = (\delta X_0/\lambda, 0)$  and terminates at  $(0, 0)$ , corresponds to the travelling wave shown in Figure 1 and has been drawn using a heavy solid line. The eigenvector in (3.3) and its negative are shown near the stable node at  $(0, 0)$ , and the arrows indicate the direction along the trajectory with increasing  $\xi$ . Similarly, the two eigenvalues in (3.4) and their negatives are shown at the saddle point  $(\delta X_0/\lambda, 0)$ , and they form the separatrices of the saddle, close to this point.

#### 4. The nonadiabatic case

In this section, the previous asymptotic analysis is applied to the situation in which an additional cooling term is added to the energy equation in the system (2.5)–(2.6). Simple Newtonian cooling is assumed, so that the new system of nondimensional equations takes the form

$$\frac{\partial X}{\partial t} = \sigma \frac{\partial^2 X}{\partial x^2} - \alpha \mu X k_1(T) - \mu X k_2(T), \quad (4.1)$$

$$\frac{\partial T}{\partial t} = \frac{\partial^2 T}{\partial x^2} - \alpha \gamma X k_1(T) + X k_2(T) - \beta(T - \theta_a). \quad (4.2)$$

Here it is assumed in addition that the ambient temperature  $\theta_a$  is equal to the ignition temperature, for simplicity. The new parameter  $\beta$  is therefore the rate of Newtonian cooling to ambient.

If again the asymptotic approximations (2.10) are invoked, and a travelling-wave coordinate of the type (2.8) is introduced, then the nonadiabatic governing equations (4.1)–(4.2) take the form

$$-c \frac{dX}{d\xi} = -\lambda X T_1, \quad -c \frac{dT_1}{d\xi} = \frac{d^2 T_1}{d\xi^2} + \delta X T_1 - \beta T_1, \quad (4.3)$$

in which the combination parameters  $\lambda$  and  $\delta$  are as in (2.12).

Unlike the purely adiabatic system considered in Section 2, this new system (4.3) no longer reduces to a phase-plane system for the temperature  $T_1$  but remains irreducibly third order in that variable. However, the first equation in the system (4.3) can be written so as to eliminate the temperature variable  $T_1$  in terms of the mass fraction  $X$ , and gives

$$T_1 = \frac{c}{\lambda} \frac{d}{d\xi} (\ln X). \quad (4.4)$$

Now the second equation in the system (4.3) can be integrated at once to yield

$$-c T_1 = \frac{dT_1}{d\xi} + \frac{c\delta}{\lambda} (X - X_0) - \frac{c\beta}{\lambda} \ln\left(\frac{X}{X_0}\right),$$

using the unburnt conditions  $X \rightarrow X_0$  and  $T_1 \rightarrow 0$  as  $\xi \rightarrow \infty$  ahead of the flame. Finally, the variable  $T_1$  in this equation can be eliminated using (4.4), and the result is a second-order differential equation for the mass fraction  $X$ . This may be expressed as

$$\frac{dX}{d\xi} = G, \quad \frac{dG}{d\xi} = -\delta X (X - X_0) + \beta X \ln\left(\frac{X}{X_0}\right) - cG + \frac{G^2}{X}. \quad (4.5)$$

Once again, a phase-plane system has been obtained, although now for the mass fraction  $X$ , rather than the temperature  $T_1$ . This again admits a rather complete analysis, complementing that presented in Section 3. Finally, temperature is recovered from equation (4.4) in the simple form

$$T_1 = \frac{cG}{\lambda X}. \quad (4.6)$$

The steady states of the phase-plane system (4.5) occur at the three points  $(X, G) = (0, 0)$ ,  $(X^*, 0)$  and  $(X_0, 0)$ , in which the constant  $X^*$  satisfies the nonlinear algebraic equation

$$\frac{\delta}{\beta}(X - X_0) = \ln\left(\frac{X}{X_0}\right). \quad (4.7)$$

An equation similar to this was given by Weber et al. [12], and it arose in a model of the spread of an infectious disease. It is straightforward to demonstrate that  $0 < X^* < X_0$  when  $\beta/\delta < X_0$  but that  $X^* > X_0$  if  $\beta/\delta > X_0$ . This second case is clearly unphysical, and only the first case is of practical interest, since it involves a burnt fraction  $X^*$  behind the flame front that is less than the original unburnt fraction  $X_0$ . Importantly, in the case  $\beta/\delta < X_0$  of practical interest, the fuel behind the moving flame front cannot be completely consumed since  $X^* > 0$ , unlike the purely adiabatic case considered in Section 2.

As in Section 3, the stability of the steady states is again determined by analysis of the eigenvalues of the Jacobian matrix for the phase-plane system (4.5). For the unburnt equilibrium  $(X, G) = (X_0, 0)$  ahead of the flame, the eigenvalues are easily calculated to be

$$\frac{1}{2}[-c \pm \sqrt{c^2 + 4(\beta - \delta X_0)}].$$

As previously, this must be chosen to be a degenerate stable node, in view of the form (2.9) of the rate parameters. This then determines the wave propagation speed to be

$$c = 2\sqrt{\delta X_0 - \beta}, \quad (4.8)$$

so generalizing the result (3.2) in the purely adiabatic case. The wave speed (4.8) is reduced by the presence of convective cooling, with coefficient  $\beta$ .

It now follows that the steady state  $(X, G) = (X_0, 0)$  has the behaviour

$$\text{repeated eigenvalue } -c/2, \quad \text{eigenvector } \begin{bmatrix} 1 \\ -c/2 \end{bmatrix}, \quad (4.9)$$

which is completely consistent with the adiabatic result (3.3). However, in this case there is, formally, a transcritical bifurcation at  $\beta/\delta = X_0$  which is indicated in Figure 3 with a dashed vertical line. At this point, the wave speed  $c$  in equation (4.8) changes from real to complex, so that the degenerate stable node for  $\beta/\delta < X_0$  formally becomes a centre when  $\beta/\delta > X_0$ . This is, however, of little practical concern since travelling-wave behaviour is clearly no longer possible when  $c$  is complex. The other steady

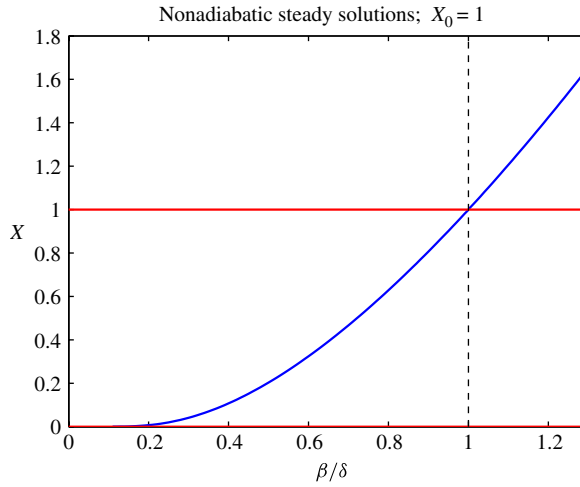


FIGURE 3. The three steady states of the nonadiabatic phase-plane system. The situation is illustrated for the case  $X_0 = 1$ , as a function of the bifurcation parameter  $\beta/\delta$ . The two red horizontal lines illustrate the solutions  $X = 0$  and  $X = X_0$ , and the blue curve corresponds to the third solution  $X^*$ . The dashed vertical line occurs at  $\beta/\delta = X_0$ . (Colour available online.)

state  $(X, G) = (X^*, 0)$  behind the flame behaves as

$$\text{eigenvalues } \frac{1}{2}(-c \pm \sqrt{c^2 + 4\Lambda}), \quad \text{eigenvectors } \left[ \frac{1}{2}(-c \pm \sqrt{c^2 + 4\Lambda}) \right], \quad (4.10)$$

in which the wave speed  $c$  is given in equation (4.8) and the constant

$$\Lambda = \beta - \delta X^*$$

has been defined for convenience.

There is a third steady-state point  $(X, G) = (0, 0)$  of the system (4.5) in the phase plane. Its behaviour is not of particular interest since it is not an achievable outcome. Nevertheless, for completeness, an analysis of this point is briefly discussed here. From inspection of the system (4.5), it is evident that the origin is a singular point, so that linearization about this point is not possible. To proceed, the system (4.5) is written as a single second-order equation, and the mass fraction  $X$  is considered in the form

$$X = X_0 e^W. \quad (4.11)$$

The statement  $X \rightarrow 0$  is equivalent to  $W \rightarrow -\infty$ . Under the transformation (4.11), the second-order differential equation for  $X$  becomes

$$\frac{d^2 W}{d\xi^2} + c \frac{dW}{d\xi} - \beta W = -\delta X_0 (e^W - 1),$$

and as  $W \rightarrow -\infty$ , this equation is asymptotically equivalent to

$$\frac{d^2W}{d\xi^2} + c \frac{dW}{d\xi} - \beta W = \delta X_0.$$

This is a linear differential equation with general solution

$$W(\xi) = -K_1 e^{\Gamma_1 \xi} - K_2 e^{\Gamma_2 \xi} - \frac{\delta}{\beta} X_0, \quad (4.12)$$

in which  $K_1$  and  $K_2$  are arbitrary (positive) constants and

$$\Gamma_1 = \frac{1}{2}[-c + \sqrt{c^2 + 4\beta}], \quad \Gamma_2 = \frac{1}{2}[-c - \sqrt{c^2 + 4\beta}].$$

The situation  $W \rightarrow -\infty$  is of interest here, and the general solution (4.12) shows that this may come about in one of two ways. Firstly, if  $\xi \rightarrow -\infty$  then it is appropriate to take

$$W(\xi) \rightarrow -K_2 e^{\Gamma_2 \xi}.$$

Secondly, if  $\xi \rightarrow \infty$  then

$$W(\xi) \rightarrow -K_1 e^{\Gamma_1 \xi}.$$

When these results are combined with the transformation (4.11), it is evident that trajectories in the  $(X, G)$  phase plane return to the point  $(0, 0)$  at an exponentially rapid rate. In the phase plane the trajectories may thus be shown to have the behaviour

$$\begin{aligned} G &\sim \Gamma_2 X \ln\left(\frac{X}{X_0}\right) & \text{if } \xi \rightarrow -\infty, \\ G &\sim \Gamma_1 X \ln\left(\frac{X}{X_0}\right) & \text{if } \xi \rightarrow \infty, \end{aligned}$$

after some algebra. Thus trajectories in the phase plane enter the point  $(0, 0)$  vertically, either from above if  $\xi \rightarrow \infty$  or from below if  $\xi \rightarrow -\infty$ .

Sample results are shown here for the case  $\alpha = 1/2$ ,  $\mu = 1$ ,  $\gamma = 1$ ,  $\epsilon = 3/2$  and unburnt mass fraction  $X_0 = 1$ , as in Section 3. In addition, the cooling rate to ambient is chosen to be  $\beta = 0.1$ . From equation (4.8), the wave speed is calculated to be  $c = 0.7746$ , and the burnt fraction behind the wave is computed from equation (4.7) by Newton's method to be  $X^* = 0.1074$ . Figure 4(a) shows the mass fraction for the travelling wave, and unlike the similar diagram in Figure 1 in the adiabatic case, the mass is not all consumed by the flame, but instead  $X \rightarrow X^*$  for large negative  $\xi$ . The temperature pulse is calculated using equation (4.6), and is shown in Figure 4(b). Unlike the adiabatic temperature profile shown in Figure 1(a), here the perturbation temperature  $T_1$  behind the flame now returns to zero. Thus the physical temperature  $T$  regains the ambient value  $\theta_a$  behind the flame, as must occur when Newtonian cooling at rate  $\beta$  is incorporated into the model.

The  $(X, G)$  phase plane for the nonadiabatic case is shown in Figure 5, for the same case as illustrated in Figure 4. The travelling wave is shown as a thick solid curve

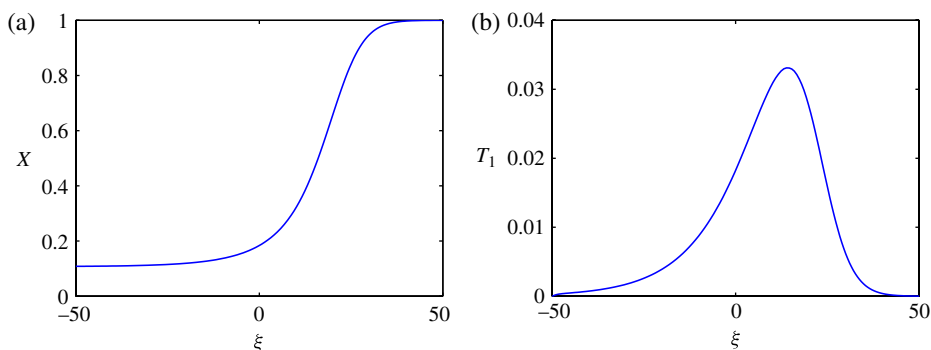


FIGURE 4. (a) Mass fraction and (b) temperature profile for a travelling wave, with parameters as given in the text.

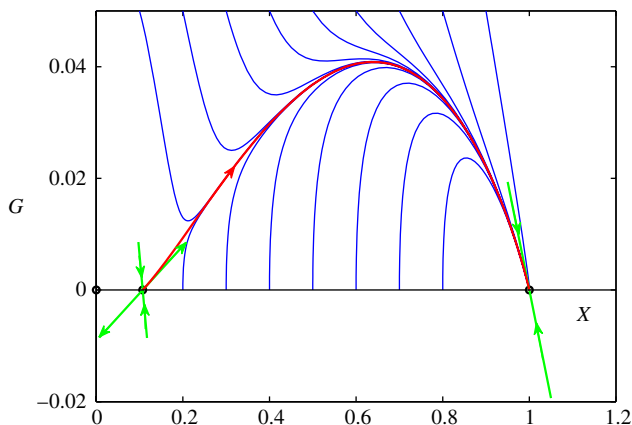


FIGURE 5. The nonadiabatic solution in the  $(X, G)$  phase plane. The three steady states are indicated by thick black circles. There is a saddle at  $(X^*, 0)$  and the travelling wave, indicated with a red heavy solid line, forms a connection between it and the degenerate stable node at  $(X_0, 0)$ . The eigenvectors are shown with green arrows from these two points. Other contours not associated with the travelling wave are also shown, in blue. (Colour available online.)

that connects the saddle at  $(X, G) = (X^*, 0)$  with the degenerate stable node at  $(X_0, 0)$ . A number of solution contours not directly associated with the travelling wave are sketched using thin solid lines, and they are all eventually drawn into the stable node at  $(X_0, 0)$ . These solution curves were obtained by numerical integration of the system (4.5). The eigenvectors (4.9) and (4.10) are also drawn on the phase plane in Figure 5, near the appropriate points.

## 5. Conclusion

In this note, an asymptotic approximation has been given to the full fourth-order equations that describe the travelling wave in a competitive endothermic–exothermic

$$\alpha = 0.5; \mu = 1; \gamma = 1; \varepsilon = 3/2; X_0 = 1; \beta = 0.1$$

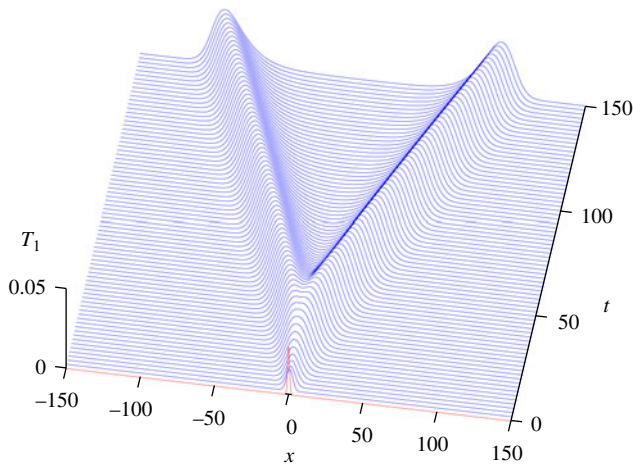


FIGURE 6. Numerical solution of the full system of partial differential equations for the nonadiabatic system. The initial temperature was a simple Gaussian profile, shown in red, and the behaviour of the temperature profile in space  $x$  is displayed for 75 different times, over  $0 < t < 150$ . (Colour available online.)

reaction system. By ignoring the effects of material diffusion, appropriate to a solid fuel system, the equations are reduced to third order, and then by approximating the Arrhenius-like temperature-dependent reaction rates, the system is integrated to give a second-order equation for the temperature perturbation  $T_1$  in the purely adiabatic case. This then admits a full analysis in the phase plane, which is reasonably straightforward to undertake. The key results of this asymptotic analysis are that an explicit formula is obtained for the propagation speed of the travelling wave front, along with the condition  $\delta > 0$  required for such a wave to exist. The results obtained are nevertheless in agreement with more complex combustion models.

When Newtonian cooling to ambient temperature is readmitted to the model, a simple phase-plane analysis for temperature is no longer possible. However, the equation for the burnt mass fraction  $X$  of the fuel can still be integrated to give a phase-plane system, when the Arrhenius reaction rates are subject to the same asymptotic approximation as previously. The wave speed is again available in a simple closed-form expression, and a rather complete analysis of the system is possible.

As an independent check on the reliability of the asymptotic approximations made in this paper, the original partial differential equations (4.1)–(4.2) have been solved numerically using the method of lines, with rate functions (2.9). A grid of 1501 mesh points was placed equally spaced along the  $x$ -axis, over the interval  $-150 < x < 150$ , and the equations discretized in space were integrated forward in time using Matlab. The mass fraction was set initially to the value  $X(x, 0) = X_0$  and the initial temperature was taken to be a simple Gaussian profile,  $T_1(x, 0) = 0.03 \exp(-x^2)$ . A solution is shown in Figure 6, for the same values of the parameters as in Figures 4 and 5. As time

progresses, two wave fronts develop, each moving away from the site of the original disturbance. Their profiles slowly approach a time-independent shape moving at a constant speed, and the shape matches closely that shown in Figure 4(b). The unburnt fraction remaining in the portion between the two outwardly moving fronts in Figure 6 approaches the value  $X^* = 0.1074$  obtained in Section 4. It is more difficult to estimate the wave speed that is approached by the fronts in Figure 6 for large times, from the numerical solution of the full system (4.1)–(4.2), although the average speed over the time interval  $100 < t < 150$  is about  $c \approx 0.74$ , which is in reasonable agreement with the value  $c = 0.7746$  calculated from equation (4.8). A comparison such as this gives confidence in the asymptotic analysis presented here.

### Acknowledgement

The author is indebted to two anonymous referees for constructive criticism of this manuscript.

### References

- [1] R. Ball, A. C. McIntosh and J. Brindley, “Thermokinetic models for simultaneous reactions: a comparative study”, *Combust. Theory Model.* **3** (1999) 447–468; doi:10.1088/1364-7830/3/3/302.
- [2] J. Brindley, J. F. Griffiths, A. C. McIntosh and J. Zhang, “Initiation of combustion waves in solids, and the effects of geometry”, *ANZIAM J.* **43** (2001) 149–163; doi:10.1017/S1446181100011482.
- [3] L. K. Forbes, “A two-dimensional model for large-scale bushfire spread”, *J. Aust. Math. Soc. Ser. B* **39** (1997) 171–194; doi:10.1017/S0334270000008791.
- [4] L. K. Forbes and W. Derrick, “A combustion wave of permanent form in a compressible gas”, *ANZIAM J.* **43** (2001) 35–58; doi:10.1017/S144618110001141X.
- [5] B. F. Gray, S. Kalliadasis, A. Lazarovici, C. Macaskill, J. H. Merkin and S. K. Scott, “The suppression of an exothermic branched-chain flame through endothermic reaction and radical scavenging”, *Proc. R. Soc. Lond. A* **458** (2002) 2119–2138; doi:10.1098/rspa.2002.0961.
- [6] P. Gray and S. K. Scott, *Chemical oscillations and instabilities: non-linear chemical kinetics* (Clarendon Press, Oxford, 1994).
- [7] A. Hmadi, A. C. McIntosh and J. Brindley, “A mathematical model of hotspot condensed phase ignition in the presence of a competitive endothermic reaction”, *Combust. Theory Model.* **14** (2010) 893–920; doi:10.1080/13647830.2010.519050.
- [8] B. J. Matkowsky and G. I. Sivashinsky, “Propagation of a pulsating reaction front in solid fuel combustion”, *SIAM J. Appl. Math.* **35** (1978) 465–478; doi:10.1137/0135038.
- [9] J. D. Murray, *Mathematical biology* (Springer, Berlin, 1989).
- [10] J. J. Sharples, H. S. Sidhu, A. C. McIntosh, J. Brindley and V. V. Gubernov, “Analysis of combustion waves arising in the presence of a competitive endothermic reaction”, *IMA J. Appl. Math.* **77** (2012) 18–31; doi:10.1093/imamat/hxr072.
- [11] R. O. Weber, G. N. Mercer, H. S. Sidhu and B. F. Gray, “Combustion waves for gases ( $Le = 1$ ) and solids ( $Le \rightarrow \infty$ )”, *Proc. R. Soc. Lond. A* **453** (1997) 1105–1118; doi:10.1098/rspa.1997.0062.
- [12] R. O. Weber, G. N. Mercer and H. S. Sidhu, “Combustion leftovers”, *Math. Comput. Model.* **36** (2002) 371–377; doi:10.1016/S0895-7177(02)00131-0.
- [13] Ya. B. Zel’dovich, G. I. Barenblatt, V. B. Librovich and G. M. Makhviladze, *Mathematical theory of combustion and explosions* (Plenum Press, New York, 1985).